ChemComm

COMMUNICATION

View Article Online
View Journal | View Issue

Cite this: *Chem. Commun.*, 2019, 55, 7918

Received 1st June 2019,
Accepted 11th June 2019

DOI: 10.1039/c9cc04222a

rsc.li/chemcomm

A heavy metal-free $CuInS_2$ quantum dot sensitized NiO photocathode with a Re molecular catalyst for photoelectrochemical CO_2 reduction†

Jing Huang,‡[a] Bo Xu,[a] Lei Tian,[a] Palas Baran Pati,[a] Ahmed S. Etman,[b] Junliang Sun,[b] Leif Hammarström[a] and Haining Tian *[a]

Heavy metal-free $CuInS_2$ quantum dots (QDs) were employed as a photosensitizer on a NiO photocathode to drive an immobilized molecular Re catalyst for photoelectrochemical CO_2 reduction for the first time. A photocurrent of 25 μA cm^{-2} at −0.87 V *vs.* NHE was obtained, providing a faradaic efficiency of 32% for CO production.

Dye-sensitized solar fuel devices (DSSFDs)[1–4] have recently become an attractive and challenging research topic due to their advantage of low-cost solar fuel production. A typical DSSFD[5] consists of a photoanode and a photocathode based on nano-porous electrodes with large band gap n-type and p-type semiconductors, respectively, decorated with photosensitizers and molecular catalysts. Using large band gap semiconductors electrodes can effectively extract charges from an excited photosensitizer to form a reduced/oxidized photosensitizer which normally has a longer lifetime than its excited state, thus facilitating catalyst reduction/oxidation. The dye-sensitized photocathode is where reduction reactions such proton reduction and CO_2 reduction take place. Development of the photocathode is therefore important for the overall performance and fuel products of a DSSFD.

CO_2 reduction is an attractive process, as it in principle can produce highly valuable carbon-based fuels and use of these fuels does not break the balance of CO_2 in the atmosphere. Few works have been done on dye-sensitized photocathodes for light driven CO_2 reduction.[6–13] Armstrong and co-workers[7] reported an organic dye P1 sensitized NiO photocathode using an enzyme (carbon monoxide dehydrogenase I) as a catalyst to realize light driven CO_2 reduction into CO. Since the molecular Re bipyridine catalyst is easy to synthesize, shows good selectivity of CO product and can also be operated in the presence of O_2, scientists have been attempting to use the Re catalyst on dye sensitized photocathodes. However, CO_2 reduction potentials of the Re catalysts are normally located *ca.* −1.0 V *vs.* NHE, which requires photosensitizers having a more negative potential in order to drive the reduction of the Re catalyst. In 2014, Inoue and co-workers[6] reported a porphyrin–Re catalyst covalently linked system on a NiO photocathode showing light driven CO_2 reduction. Subsequently, both Meyer's[10,11,14] and Ishitani's[8,9,12,13] teams showed the possibilities to use Ru complexes to drive the Re catalyst through different arrangements such as supramolecular, covalent linkage and cross-linkage on NiO- or $CuGuO_2$[9]-based photocathodes. As the photosensitizer is one of the key components in the photocathodes exhibiting light harvesting and charge generation/transfer, seeking other suitable photosensitizers to drive CO_2 reduction catalysts is therefore desirable.

Quantum dots (QDs) have large absorption coefficients,[15] bandgap and band position tunability,[16] and rich surface properties.[17] CdSe QD sensitized NiO photocathodes[18,19] have shown superior performance to molecular dye-based systems[20–26] for light driven proton reduction in the presence of a molecular catalyst. Inspired by this background, we were motivated to build up a QD-based photocathode for CO_2 reduction. Considering the toxicity issue, we chose a heavy metal-free $CuInS_2$ QD as the photosensitizer to sensitize a NiO photocathode (see Fig. 1). $CuInS_2$ QDs have been used as photosensitizers in a few hybrid photocatalytic systems for both proton and CO_2 reduction with high activity,[27–30] indicating that $CuInS_2$ QDs are a type of good photosensitizers in photocatalytic systems. Moreover, we have recently proved that the Re catalyst can be ultrafast reduced by $CuInS_2$ QDs and produce CO in a dispersed system.[31] Eventually, the heavy-metal free $CuInS_2$ QD sensitized NiO photocathode for the first time showed CO_2 reduction reactivity after being co-immobilized using a Re catalyst.

The water soluble colloidal $CuInS_2$ QDs were directly synthesized from an aqueous solution, with moderate modification of a reported method.[32] Briefly, instead of employing L-glutathione (GSH) as a capping ligand in the original synthesis protocol, we

[a] *Department of Chemistry-Ångström Laboratory, Uppsala University, Box 523, SE 751 20, Uppsala, Sweden. E-mail: haining.tian@kemi.uu.se*
[b] *Department of Materials and Environmental Chemistry (MMK), Stockholm University, SE 106 91 Stockholm, Sweden*

† Electronic supplementary information (ESI) available. See DOI: 10.1039/c9cc04222a

‡ Current address: Department of Applied Physics, School of Engineering Sciences, KTH-Royal Institute of Technology, Stockholm, Sweden.

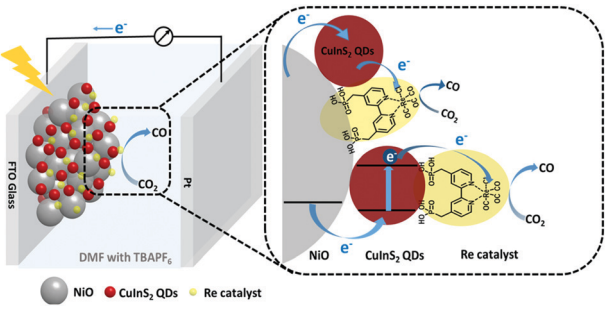

Fig. 1 Configuration of a PEC cell for CO_2 reduction based on the NiO photocathode co-grafted with the $CuInS_2$ QDs and the Re catalyst, and illustration of electron injection and hole transfer in the photocathode.

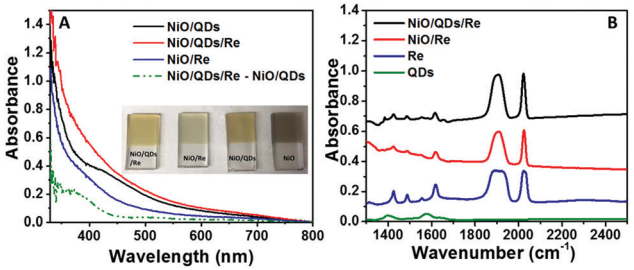

Fig. 2 (A) Absorption spectra of NiO photocathodes immobilized with $CuInS_2$ QDs (NiO/QDs), Re catalyst (NiO/Re), and both QDs and Re catalyst (NiO/QDs/Re) (absorption of the NiO substrate has been subtracted), respectively. Inset: Image of the corresponding photocathodes. (B) FTIR spectra of NiO/QD/Re and NiO/Re electrodes, as well as pure $CuInS_2$ QDs and the Re catalyst.

utilized L-cysteine for our QDs. Since L-cysteine has a smaller molecular size than GSH, the prepared QDs can penetrate the NiO mesoporous film more easily. More importantly, using GSH as the capping ligand made the QD aqueous solution destroy the mesoporous NiO substrate; however, the reason for this phenomenon is not clear at this moment, probably due to some unexpected reactions occurring between NiO and GSH. Replacement of GSH with L-cysteine can completely avoid this problem. From the X-ray diffraction (XRD) pattern (Fig. S1B, ESI†), one can conclude that our as-synthesized $CuInS_2$ QDs can be indexed into the chalcopyrite phase or the zinc blende phase of $CuInS_2$. Considering that the synthesized $CuInS_2$ QDs in this work were off-stoichiometric, the structure of the QDs was therefore zinc blende phase.[29,33] From the high-resolution transmission electron microscopy (HRTEM) image (Fig. S1A, ESI†), we can find that the size of the QDs was around 4 nm, and the lattice can be indexed to the (111) facet of zinc blende $CuInS_2$. The absorption onset of the obtained QDs was 700 nm (Fig. S1C, ESI†) with a weak shoulder around 550 nm, and the corresponding bandgap was determined to be 2.45 eV (Fig. S2, ESI†).

The as-synthesized $CuInS_2$ QDs were then immobilized on a mesoporous NiO electrode (thickness of 1 μm, Fig. S3, ESI†) by immersing the electrode in a QD stock solution under an ambient environment. Benefiting from the carboxylic acid unit in the cysteine ligand, our water soluble $CuInS_2$ QDs can easily attach onto the NiO electrode, and the color of the electrode turned yellowish after being sensitized by QDs, as demonstrated in Fig. 2. Simultaneously, we can also see that the absorption feature of the $CuInS_2$ QD sensitized NiO electrode (NiO/QDs) resembled that of QDs in solution, implying that there was no obvious change or aggregation of QDs after they were grafted onto the NiO electrode. Moreover, the absorbance of our QD sensitized electrode (after subtracting the bare NiO background) reached 0.4 at 400 nm, which was comparable with that of a dye-sensitized NiO photocathode.[34,35] It is commonly believed that poor deposition of colloidal QDs on a NiO substrate greatly limits the performance of the QD sensitized NiO photocathode.[18,36] The calculated concentration of the colloidal $CuInS_2$ QDs in our NiO/QDs electrode was around 6.7 mM (see calculation details in Table S1, ESI†), which was almost double the concentration of CdSe QDs prepared by the OPAR method from the reported work with excellent performance in hydrogen evolution.[18] The high loading concentration of the $CuInS_2$ QDs indicates that the size and surface properties of our QDs were favorable for them to immobilize onto the NiO electrode, and our modified synthetic approach might provide a feasible way to obtain colloidal $CuInS_2$ QDs which are suitable for sensitizing mesoporous NiO photocathodes. For immobilizing a catalyst onto the electrodes, the QD sensitized NiO photoelectrodes were further immersed in the Re catalyst (the molecular structure shown in Fig. 1 and Fig. S5, ESI†) solution. Thanks to the phosphonic acid groups, the Re catalyst can also efficiently assemble on the QD sensitized NiO electrode. With the Re catalyst, the absorption of the photocathode around 400 nm (NiO/QDs/Re) obviously increased, owing to the intensive absorption of the Re catalyst in that region. The differential absorption spectrum between the NiO/QDs/Re electrode and the NiO/QDs electrode (green dotted line in Fig. 2) clearly matches the absorption spectrum of a pure Re catalyst in ethanol (Fig. S4, ESI†). Fig. 2B shows the Fourier-transform infrared (FTIR) spectra of samples scraped off from the electrodes, together with those of a pure Re catalyst and QDs. Both the samples from NiO/Re and NiO/QDs/Re electrodes exhibit absorption peaks at 1890, 1921 and 2022 cm^{-1}, which are consistent with the pure Re catalyst, and can be assigned to the ν_{CO} stretches from the catalyst molecule.[31,37,38] These results suggest that the Re catalyst has been successfully immobilized onto the QD sensitized NiO electrodes. By comparison of the UV-vis absorption spectra of the Re ethanol solution before and after immobilizing the NiO/QD electrode, the concentration of the Re catalyst on the NiO/QDs/Re electrode was estimated to be 8.2 nmol cm^{-2}. SEM images (Fig. 3) show that the NiO electrode became rougher after being co-sensitized by the QDs and the Re catalyst, as compared with the blank NiO electrode (Fig. S3, ESI†). From the HRTEM image of the sensitized electrode (Fig. 3B), we can find both the lattices from NiO(111) and $CuInS_2$(111) QDs. Mapping of elements in the electrode shows that $CuInS_2$ QDs and Re catalyst were uniformly dispersed inside the electrode.

The proposed working principle of the photocathode for CO_2 reduction is illustrated in Fig. 1. The valence band (VB) of NiO is normally reported to be 0.5 V *vs.* NHE (hereafter all potential values are reported *vs.* NHE).[39] According to the size

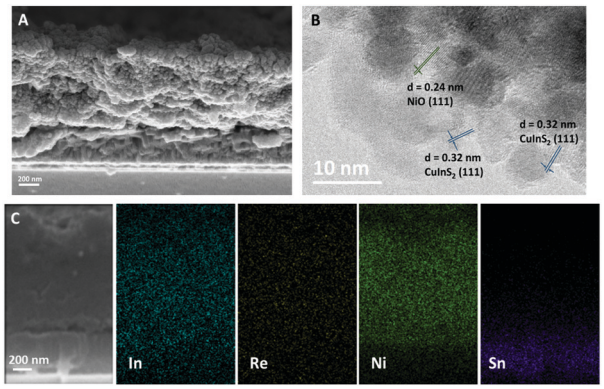

Fig. 3 SEM image (A) of the NiO/QD/Re electrode, with corresponding EDX element mapping analysis in a selected SEM cross section range on the electrode (C). (B) HRTEM image of the sample scratched from the photocathode.

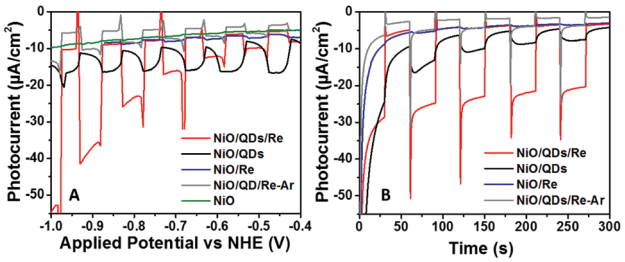

Fig. 4 Linear sweep voltammetry (LSV) plots of a NiO photocathode based on different samples under chopped light irradiation (A). Without any specification, the measurements were conducted in a CO_2 atmosphere. (B) Chopped-light chronoamperograms of the photocathodes at an applied bias of −0.87 V *vs.* NHE.

(4 nm) and Cu/In ratio (3/20) of the as-synthesized $CuInS_2$ QDs, the conduction band (CB) of the QDs is estimated to be located at −1.3 V, and the VB is about 1.05 V[29]. Thermodynamically, the $CuInS_2$ QDs can inject holes into the VB of NiO under illumination. Fig. S6 (ESI†) shows that when the QD sensitized NiO electrode was included in a three-electrode system with pentaaminechlorocobalt(III) chloride as a sacrificial electron acceptor, a photocurrent of up to 400 μA cm^{-2} was obtained, while no obvious photocurrent was observed from the bare NiO electrode. The high photocurrent indicates that holes from the excited $CuInS_2$ QDs can indeed transfer to the NiO electrode and the electrons can be captured by the electron acceptor. Simultaneously, the CB of the $CuInS_2$ QDs is more negative compared to the first reductive potential of the Re catalyst,[31] implying that the photo-induced electron transfer from the $CuInS_2$ QDs to the Re catalyst is also thermodynamically feasible. As shown in Fig. S7 (ESI†), the fluorescence of the $CuInS_2$ QDs was quenched gradually upon addition of the Re catalyst in the QD solution, suggesting that there is electron transfer from the $CuInS_2$ QDs to the Re catalyst. Our previous results also confirmed that there is an ultrafast electron transfer from the $CuInS_2$ QDs to the Re catalyst even when the CB of QDs was slightly more negative compared to the reduction potential of the Re catalyst.[31] Based on these results, we suggest that the transfer of photo-generated electrons from the QDs to the Re catalyst for CO_2 reduction on the NiO electrode is energetically possible.

The $CuInS_2$ QD and Re-catalyst co-grafted NiO photocathode was then employed in a three-electrode PEC system to evaluate its performance in photoelectrochemical CO_2 reduction. As shown in Fig. 4A, there was no obvious photocurrent observed from a blank NiO electrode, indicating that the NiO electrode cannot perform CO_2 reduction on its own. When the NiO electrode was sensitized by the $CuInS_2$ QDs (NiO/QDs), a photocurrent of *ca.* 10 μA cm^{-2} was generated, which decreased gradually when the applied bias was increased. The rapid response of the photocurrent to the chopped light suggests that the electron–hole pairs in $CuInS_2$ QDs could efficiently separate under illumination; however, gradually decreased photocurrent implies that direct electron transfer from QDs to CO_2 is inefficient, inducing substantial recombination of electrons and holes in the NiO electrode. Only negligible photocurrent could be measured from the Re catalyst grafted NiO electrode without QDs (NiO/Re), owing to slight visible absorption of the Re catalyst. When the QD sensitized electrode was immobilized with the Re catalyst (NiO/QDs/Re, red traces in Fig. 4), a significant enhancement of photocurrent was obtained, and the photocurrent increased when a more negative bias potential was applied. The improved photocurrent in the presence of both QDs and catalyst on the electrode strongly implies that there is electron transfer from the QDs to the Re catalyst and the system works for CO_2 reduction as well. Therefore, charge recombination in the photocathode is significantly suppressed, and the photocurrent is enhanced. For comparison, the NiO/QD/Re electrode was also evaluated in the presence of argon instead of CO_2. As indicated by the grey curve in Fig. 4, the generated photocurrent was much smaller than that of the same electrode with CO_2 in the system. This phenomenon confirms that the electrons generated in QDs can indeed go to CO_2 through the Re catalyst, and then realizes the whole photocatalytic reaction. Compared to the DSSFD systems for CO_2 reduction, our $CuInS_2$ QDs sensitized system has shown comparable photocurrent (Table S2, ESI†), implying that $CuInS_2$ QDs can be a desirable photosensitizer for photoelectrochemical CO_2 reduction with molecular catalysts. The long-term stability of the co-grafted photocathode was evaluated by subjecting it to irradiation up to 100 min, and the result is shown in Fig. S8A (ESI†). Though the photocurrent was rather stable during the first 300 s (Fig. 4B), the current decreased gradually upon illumination. Eventually, only CO product was detected in the system under 100 min of illumination with a faradaic efficiency (FE) of 32% for CO_2 reduction. No hydrogen was detected. The low FE could be caused by the undetectable CO in the electrolyte or other side reactions such as reduction of residual O_2. Notably, no CO could be detected in the same system with Ar (NiO/QDs/Re–Ar, Fig. S8B, ESI†), indicating that the detected CO in the PEC system with CO_2 (NiO/QDs/Re–CO_2) must come from the reduction of CO_2, rather than decomposition of the Re catalyst. Moreover, the turnover number (TON, defined as the number of moles of CO that a mole of

catalyst converts) of the system was 11, which further confirms that the detected CO should not result from decomposition of the Re catalyst.

In summary, heavy metal-free $CuInS_2$ QDs as a photosensitizer and a Re molecular catalyst have been successfully employed to co-sensitize a NiO photocathode for CO_2 reduction for the first time. UV-vis absorption spectra and SEM images prove that our $CuInS_2$ QDs synthesized by a modified reported method can be easily immobilized onto the NiO mesoporous substrate and provide a high loading efficiency. The prepared photocathode was able to photoelectrochemically reduce CO_2 into CO with a FE of 32%. The performance of the QD photocathode could be improved by optimizing the configuration of the electrode, for example, by introduction of an Al_2O_3–ALD layer in the interfaces to further suppress the charge recombination in the device as well as to prevent desorption of the QDs and the catalyst.[35] More effort will be devoted to further improvement of the photocurrent stability and enhancement of FE in the following work.

This work was supported by the Göran Gustafsson Foundation, the Olle Engkvist Byggmästare Foundation and the Swedish Energy Agency (grant 11674-8). Lei Tian acknowledges the support from the China Scholarship Council. We also greatly thank Prof. Marc Fontecave for valuable discussions and Prof. Sascha Ott for providing access to synthetic lab and GC test.

Conflicts of interest

There are no conflicts to declare.

Notes and references

1 H. Tian, *ChemSusChem*, 2015, **8**, 3746–3759.
2 Z. Yu, F. Li and L. Sun, *Energy Environ. Sci.*, 2015, **8**, 760–775.
3 E. A. Gibson, *Chem. Soc. Rev.*, 2017, **46**, 6194–6209.
4 D. L. Ashford, M. K. Gish, A. K. Vannucci, M. K. Brennaman, J. L. Templeton, J. M. Papanikolas and T. J. Meyer, *Chem. Rev.*, 2015, **115**, 13006–13049.
5 F. Li, K. Fan, B. Xu, E. Gabrielsson, Q. Daniel, L. Li and L. Sun, *J. Am. Chem. Soc.*, 2015, **137**, 9153–9159.
6 Y. Kou, S. Nakatani, G. Sunagawa, Y. Tachikawa, D. Masui, T. Shimada, S. Takagi, D. A. Tryk, Y. Nabetani, H. Tachibana and H. Inoue, *J. Catal.*, 2014, **310**, 57–66.
7 A. Bachmeier, S. Hall, S. W. Ragsdale and F. A. Armstrong, *J. Am. Chem. Soc.*, 2014, **136**, 13518–13521.
8 G. Sahara, R. Abe, M. Higashi, T. Morikawa, K. Maeda, Y. Ueda and O. Ishitani, *Chem. Commun.*, 2015, **51**, 10722–10725.
9 H. Kumagai, G. Sahara, K. Maeda, M. Higashi, R. Abe and O. Ishitani, *Chem. Sci.*, 2017, **8**, 4242–4249.
10 D. Wang, Y. Wang, M. D. Brady, M. V. Sheridan, B. D. Sherman, B. H. Farnum, Y. Liu, S. L. Marquard, G. J. Meyer, C. J. Dares and T. J. Meyer, *Chem. Sci.*, 2019, **10**, 4436–4444.
11 T.-T. Li, B. Shan and T. J. Meyer, *ACS Energy Lett.*, 2019, **4**, 629–636.
12 R. Kamata, H. Kumagai, Y. Yamazaki, G. Sahara and O. Ishitani, *ACS Appl. Mater. Interfaces*, 2019, **11**, 5632–5641.
13 G. Sahara, H. Kumagai, K. Maeda, N. Kaeffer, V. Artero, M. Higashi, R. Abe and O. Ishitani, *J. Am. Chem. Soc.*, 2016, **138**, 14152–14158.
14 B. Shan, S. Vanka, T.-T. Li, L. Troian-Gautier, M. K. Brennaman, Z. Mi and T. J. Meyer, *Nat. Energy*, 2019, **4**, 290–299.
15 C. Xia, W. Wu, T. Yu, X. Xie, C. van Oversteeg, H. C. Gerritsen and C. de Mello Donega, *ACS Nano*, 2018, **12**, 8350–8361.
16 L. Brus, *J. Phys. Chem.*, 1986, **90**, 2555–2560.
17 K. E. Roelofs, T. P. Brennan and S. F. Bent, *J. Phys. Chem. Lett.*, 2014, **5**, 348–360.
18 P. Meng, M. Wang, Y. Yang, S. Zhang and L. Sun, *J. Mater. Chem. A*, 2015, **3**, 18852–18859.
19 T. P. A. Ruberu, Y. Dong, A. Das and R. Eisenberg, *ACS Catal.*, 2015, **5**, 2255–2259.
20 L. Li, L. Duan, F. Wen, C. Li, M. Wang, A. Hagfeldt and L. Sun, *Chem. Commun.*, 2012, **48**, 988–990.
21 P. B. Pati, L. Zhang, B. Philippe, R. Fernández-Terán, S. Ahmadi, L. Tian, H. Rensmo, L. Hammarström and H. Tian, *ChemSusChem*, 2017, **10**, 2480–2495.
22 N. Kaeffer, J. Massin, C. Lebrun, O. Renault, M. Chavarot-Kerlidou and V. Artero, *J. Am. Chem. Soc.*, 2016, **138**, 12308–12311.
23 L. J. Antila, P. Ghamgosar, S. Maji, H. Tian, S. Ott and L. Hammarström, *ACS Energy Lett.*, 2016, **1**, 1106–1111.
24 J. Warnan, J. Willkomm, Y. Farré, Y. Pellegrin, M. Boujtita, F. Odobel and E. Reisner, *Chem. Sci.*, 2019, **10**, 2758–2766.
25 N. Põldme, L. O'Reilly, I. Fletcher, J. Portoles, I. V. Sazanovich, M. Towrie, C. Long, J. G. Vos, M. T. Pryce and E. A. Gibson, *Chem. Sci.*, 2019, **10**, 99–112.
26 K. A. Click, D. R. Beauchamp, Z. Huang, W. Chen and Y. Wu, *J. Am. Chem. Soc.*, 2016, **138**, 1174–1179.
27 S. Lian, M. S. Kodaimati and E. A. Weiss, *ACS Nano*, 2018, **12**, 568–575.
28 S. Lian, M. S. Kodaimati, D. S. Dolzhnikov, R. Calzada and E. A. Weiss, *J. Am. Chem. Soc.*, 2017, **139**, 8931–8938.
29 X.-B. Fan, S. Yu, F. Zhan, Z.-J. Li, Y.-J. Gao, X.-B. Li, L.-P. Zhang, Y. Tao, C.-H. Tung and L.-Z. Wu, *ChemSusChem*, 2017, **10**, 4833–4838.
30 M. Sandroni, R. Gueret, K. D. Wegner, P. Reiss, J. Fortage, D. Aldakov and M. N. Collomb, *Energy Environ. Sci.*, 2018, **11**, 1752–1761.
31 J. Huang, M. G. Gatty, B. Xu, P. B. Pati, A. S. Etman, L. Tian, J. Sun, L. Hammarström and H. Tian, *Dalton Trans.*, 2018, **47**, 10775–10783.
32 Y. Chen, S. Li, L. Huang and D. Pan, *Inorg. Chem.*, 2013, **52**, 7819–7821.
33 M. Kruszynska, H. Borchert, J. Parisi and J. Kolny-Olesiak, *J. Am. Chem. Soc.*, 2010, **132**, 15976–15986.
34 B. Xu, L. Tian, A. S. Etman, J. Sun and H. Tian, *Nano Energy*, 2019, **55**, 59–64.
35 L. Tian, J. Föhlinger, Z. Zhang, P. B. Pati, J. Lin, T. Kubart, Y. Hua, J. Sun, L. Kloo, G. Boschloo, L. Hammarström and H. Tian, *Chem. Commun.*, 2018, **54**, 3739–3742.
36 H.-L. Wu, X.-B. Li, C.-H. Tung and L.-Z. Wu, *Adv. Sci.*, 2018, **5**, 1700684.
37 C. D. Windle, E. Pastor, A. Reynal, A. C. Whitwood, Y. Vaynzof, J. R. Durrant, R. N. Perutz and E. Reisner, *Chem. – Eur. J.*, 2015, **21**, 3746–3754.
38 M. D. Sampson, J. D. Froehlich, J. M. Smieja, E. E. Benson, I. D. Sharp and C. P. Kubiak, *Energy Environ. Sci.*, 2013, **6**, 3748–3755.
39 G. Boschloo and A. Hagfeldt, *J. Phys. Chem. B*, 2001, **105**, 3039–3044.